THE FASEB JOURNAL • RESEARCH • www.fasebj.org

Inhibition of hypoxia-associated response and kynurenine production in response to hyperbaric oxygen as mechanisms involved in protection against experimental cerebral malaria

Marcele F. Bastos,*,[1] Ana Carolina A. V. Kayano,*,[1] João Luiz Silva-Filho,* João Conrado K. Dos-Santos,* Carla Judice,* Yara C. Blanco,* Nathaniel Shryock,[†] Michelle K. Sercundes,[‡] Luana S. Ortolan,[‡] Carolina Francelin,[§] Juliana A. Leite,* Rafaella Oliveira,[¶] Rosa M. Elias,[‖] Niels O. S. Câmara,[‖] Stefanie C. P. Lopes,*,[¶] Letusa Albrecht,*,[#] Alessandro S. Farias,* Cristina P. Vicente,[‡] Claudio C. Werneck, Selma Giorgio,[††] Liana Verinaud,[§] Sabrina Epiphanio,[‡] Claudio R. F. Marinho,[‡‡] Pritesh Lalwani,[¶] Rogerio Amino,[§§] Julio Aliberti,[†,¶¶,2] and Fabio T. M. Costa*,[3]**

*Department of Genetics, Evolution, Microbiology, and Immunology, Laboratory of Tropical Diseases–Prof. Dr. Luiz Jacintho da Silva, [§]Department of Functional and Structural Biology, **Department of Biochemistry and Tissue Biology, and [††]Department of Animal Biology, University of Campinas, Campinas, Brazil; [†]Cincinnati Children's Hospital Medical Center, Cincinnati, Ohio, USA; [‡]Department of Clinical and Toxicological Analyses, [‖]Department of Immunology, and [‡‡]Department of Parasitology, University of São Paulo, São Paulo, Brazil; [¶]Instituto Leônidas e Maria Deane, Fundação Oswaldo Cruz, Manaus, Brazil; [#]Instituto Carlos Chagas, Fundação Oswaldo Cruz, Curitiba, Brazil; [§§]Unit of Malaria Infection and Immunity, Institut Pasteur, Paris, France; and [¶¶]Division of Extramural Activities, National Institute of Allergy and Infectious Diseases, National Institutes of Health, Bethesda, Maryland, USA

ABSTRACT: Cerebral malaria (CM) is a multifactorial syndrome involving an exacerbated proinflammatory status, endothelial cell activation, coagulopathy, hypoxia, and accumulation of leukocytes and parasites in the brain microvasculature. Despite significant improvements in malaria control, 15% of mortality is still observed in CM cases, and 25% of survivors develop neurologic sequelae for life—even after appropriate antimalarial therapy. A treatment that ameliorates CM clinical signs, resulting in complete healing, is urgently needed. Previously, we showed a hyperbaric oxygen (HBO)-protective effect against experimental CM. Here, we provide molecular evidence that HBO targets brain endothelial cells by decreasing their activation and inhibits parasite and leukocyte accumulation, thus improving cerebral microcirculatory blood flow. HBO treatment increased the expression of aryl hydrocarbon receptor over hypoxia-inducible factor 1-α (HIF-1α), an oxygen-sensitive cytosolic receptor, along with decreased indoleamine 2,3-dioxygenase 1 expression and kynurenine levels. Moreover, ablation of HIF-1α expression in endothelial cells in mice conferred protection against CM and improved survival. We propose that HBO should be pursued as an adjunctive therapy in CM patients to prolong survival and diminish deleterious proinflammatory reaction. Furthermore, our data support the use of HBO in therapeutic strategies to improve outcomes of non-CM disorders affecting the brain.—Bastos, M. F., Kayano, A. C. A. V., Silva-Filho, J. L., Dos-Santos, J. C. K., Judice, C., Blanco, Y. C., Shryock, N., Sercundes, M. K., Ortolan, L. S., Francelin, C., Leite, J. A., Oliveira, R., Elias, R. M., Câmara, N. O. S., Lopes, S. C. P., Albrecht, L., Farias, A. S., Vicente, C. P., Werneck, C. C., Giorgio, S., Verinaud, L., Epiphanio, S., Marinho, C. R. F.,

ABBREVIATIONS: AhR, aryl hydrocarbon receptor; ARNT, aryl hydrocarbon receptor nuclear translocator; ATA, atmosphere pressure; BBB, blood-brain barrier; CM, cerebral malaria; CSF, cerebrospinal fluid; C_t, cycle threshold; ECM, experimental cerebral malaria; EPCR, endothelial protein C receptor; *fl/fl*, flox/flox; HBO, hyperbaric oxygen; HIF-1α, hypoxia-inducible factor 1-α; Hmox1, heme oxygenase-1 mRNA; HO-1, heme oxygenase-1; HPRT, hypoxanthine-guanine phosphoribosyltransferase; ICAM-1, intercellular adhesion molecule-1; IDO-1, indoleamine 2,3-dioxygenase 1; iE, infected erythrocyte; Itga/b1/b2, integrin α1/β1/β2; KA, kynurenine acid; KP, kynurenine pathway; Kyn, kynurenine; LFA-1, lymphocyte function-associated antigen-1; NI, noninfected; PbA, *Plasmodium berghei* ANKA; p.i., postinfection; QA, quinolinic acid; qRT-PCR, quantitative RT-PCR; Trp, tryptophan

[1] These authors contributed equally to this work.

[2] Correspondence: Scientific Review Program, Division of Extramural Activities, National Institute of Allergy and Infectious Diseases, National Institutes of Health, Bethesda, MD, USA. E-mail: julio.aliberti@nih.gov

[3] Correspondence: Department of Genetics, Evolution, Microbiology and Immunology, Laboratory of Tropical Diseases–Prof. Dr. Luiz Jacintho da Silva, University of Campinas, UNICAMP, Rua Monteiro Lobato, 255, Campinas, SP 13083-862, Brazil. E-mail: costaftm@unicamp.br or fabiotmc72@gmail.com.br

doi: 10.1096/fj.201700844R

This article includes supplemental data. Please visit *http://www.fasebj.org* to obtain this information.

 0892-6638/18/0032-4470 © FASEB

Lalwani, P., Amino, R., Aliberti, J., Costa, F. T. M. Inhibition of hypoxia-associated response and kynurenine production in response to hyperbaric oxygen as mechanisms involved in protection against experimental cerebral malaria. FASEB J. 32, 4470–4481 (2018). www.fasebj.org

KEY WORDS: brain · aryl-hydrocarbon receptor · tryptophan metabolism · endothelial cell activation

Among malaria complications, cerebral malaria (CM) is associated with high mortality and morbidity rates, mainly in children in sub-Saharan Africa, and accounts for almost half a million deaths per year (1). Although a tremendous effort has been made toward controlling CM mortality, including numerous clinical trials of different adjunctive therapies, 18% of African children and 30% of Southeast Asian adults with CM still die. Moreover, nearly 25% of survivors develop neurologic sequelae and cognitive impairments, even after optimal antimalarial treatment (2–5).

Uncontrolled production of proinflammatory cytokines, coagulopathy, endothelial activation, and oxidative stress is often associated with poor CM outcomes (6–9). CM pathologic features also include vascular occlusion, ischemia, brain edema and hemorrhages, neuronal and endothelial damage, blood-brain barrier (BBB) dysfunction, convulsions, coma, and death (7, 10). Although the host immune response plays a pivotal role in CM pathogenesis, congestion of deep microvasculature is reported in autopsies of CM patients, as well as endothelial activation and hypoxia, which correlate to BBB breakdown in CM patients (11–14). In mice, lethal infection with *Plasmodium berghei* ANKA (PbA) is a murine model widely used for experimental CM (ECM) that shares several pathogenesis components of human CM, mostly pediatric CM (10, 15).

Administration of pressurized oxygen, also referred as hyperbaric oxygen (HBO) therapy, has been successfully used in humans in a variety of disorders, such as refractory wounds, radiation injury, and decompression sickness (16). This therapy is also able to suppress transiently the inflammatory process of ischemic trauma and improve blood flow, thus ameliorating brain disorders, such as stroke (17). We have previously demonstrated that HBO therapy, in conditions suitable for human use, protects mice against the lethal disease induced by PbA infection (18). However, the molecular mechanisms involved in the neuroprotective effect of HBO during ECM remained unknown. Here, we evaluate the mechanisms of action of HBO treatment on leukocyte and parasite accumulation in the microvasculature and hence, on cerebral blood flow. Furthermore, we assess its molecular mechanisms triggered on the brain by evaluating the expression of proteins and genes encoding adhesion molecules, hypoxia-associated response, and generation of metabolites derived from the tryptophan (Trp) metabolism.

MATERIALS AND METHODS

Ethics statement

All experiments and procedures were approved by the University of Campinas Committee for Ethics in Animal Research (1366-1 and 2200-1) and by Cincinnati Children's Hospital Medical Center Institutional Animal Care and Use Committee (2013-0144). The protocols adhered to the guidelines of the Brazilian National Council for the Control of Animal Experimentation and to the *Guide for the Care and Use of Laboratory Animals* [National Institutes of Health (NIH), Bethesda, MD, USA].

Mice and murine parasites

Female C57BL/6 mice (7–10 wk old) were purchased from the Multidisciplinary Center for Biological Investigation on Laboratory Animal Science, University of Campinas, and maintained in our specific pathogen-free animal facility. Hypoxia-inducible factor 1-α flox/flox (HIF-1$\alpha^{fl/fl}$) mice were provided by Dr. George Deepe (University of Cincinnati, Cincinnati, OH, USA) (19) and crossed with Tie2cre to generate endothelial cell conditional knockout mice for HIF-1α (Tie2cre HIF-1$\alpha^{fl/fl}$).

A cloned line of PbA was kindly provided by Dr. Laurent Rénia (Singapore Immunology Network, Agency for Science, Technology and Research, Singapore). The blood-stage forms of PbA parasites were stored in liquid nitrogen after *in vivo* passages in C57BL/6 mice, as described in refs. 15 and 18. Mice were infected intraperitoneally with 10^6 infected erythrocytes (iEs), and parasitemia and CM neurologic signs were monitored daily. ECM was defined by the presence of at least 2 of the following clinical signs of neurologic involvement: ataxia, limb paralysis, poor righting reflex, seizures, rollover, and coma.

Administration of HBO in infected mice

HBO treatment in mice was conducted as described in Blanco *et al*. (18). In brief, groups of 8–10 PbA-infected mice were exposed for 1 h daily to 100% oxygen at a pressure of 3.0 atmospheres (ATA) in a hyperbaric animal research chamber (Model HB 1300B; Sechrist, Anaheim, CA, USA) from d 0 until the day the assay was performed. The chamber was pressurized and decompressed at a rate of 0.5 ATA/min, as previously described (18). Infected mice in the control group (nonexposed) were left in an ventilated room (normal oxygen tension and normal local atmospheric pressure, ~0.98 ATA).

Real-time quantitative RT-PCR

Gene expression levels and parasite load in mouse brains were assessed by real-time quantitative RT-PCR (qRT-PCR). On d 6–7 postinfection (p.i.), when mice showed signs of ECM, PbA-infected mice were perfused intracardially with PBS using a peristaltic pump (Harvard Apparatus, Cambridge, MA, USA) to remove circulating iEs and leukocytes. Extraction of total RNA from mouse brains was performed with the RNeasy Mini Kit (Qiagen, Germantown, MD, USA). Total RNA samples (1 μg) were reverse transcribed using the oligo(dT) primer from the High Capacity cDNA Reversion Transcription Kit (Thermo Fisher Scientific, Waltham, MA, USA). The mRNA expression of intercellular adhesion molecule-1 (*Icam1*); heme oxygenase-1 (HO-1) mRNA (*Hmox1*); endothelial protein C receptor (*Epcr*); *tissue factor*; lymphocyte function-associated antigen-1 (*Lfa1*); *perforin*; indoleamine 2,3-dioxygenase 1 (*Ido1*); integrin α1 (*Itga*), β1 (*Itgb1*), and β2 (*Itgb2*); and 18S was analyzed by qRT-PCR, using iTaq Universal SYBR Green Supermix (Bio-Rad, Hercules, CA, USA). Transcripts of *Il12a*, *Il12b*, aryl hydrocarbon receptor

(*Ahr*), and *Hmox1* were also evaluated by qRT-PCR (Qiagen). The oligonucleotides used are described in Supplemental Table S1. The median cycle threshold (C_t) value and $2^{-\Delta\Delta Ct}$ method were used for relative quantification analysis, and all C_t values were normalized to the hypoxanthine-guanine phosphoribosyltransferase (HPRT) mRNA expression level. Results were expressed as means, and SD of biologic triplicates is shown compared with noninfected (NI) mice.

Immunoblotting

Mouse brain protein crude extracts were homogenized in extraction buffer [EDTA, pH 7.4, 0.01 M; Tris-HCl, pH 7.4, 0.1 mM; sodium pyrophosphate, 10 mM; sodium fluoride, 100 mM; sodium orthovanadate, 10 mM; Triton, 1%; and protease inhibitor cocktail, 1% (MilliporeSigma, St. Louis, MO, USA)]. Protein concentration was determined by the Bradford method. Protein crude extract (100 μg) was incubated at 95°C for 5 min with 1 vol Laemmli sample and submitted to electrophoretic separation on an 8% SDS-PAGE. The proteins were electrotransferred onto a nitrocellulose membrane (Bio-Rad) and incubated for 1 h with blocking solution [5% dried milk (Nestlé, Vevey, Switzerland), 50 mM PBS, pH 7.4, 150 mm NaCl, 0.1% PBS-Tween]. The transferred proteins were incubated with mAb against AhR and β-actin (all purchased from Santa Cruz Biotechnology, Dallas, TX, USA) for 12 h at 4°C and diluted at 1:1000 in a PBS-Tween solution. After washing with PBS-Tween, blots were incubated for 1 h at room temperature with peroxidase-conjugated rabbit anti-mouse secondary antibody (Zymax; Zymed Laboratories, San Francisco, CA, USA), diluted at 1:10,000. The immunoreactive blots were detected by autoradiography on Kodak film GBX2 with SuperSignal West Pico Chemiluminescence Kit (Thermo Fisher Scientific). The optical density of immunoreactive bands was determined by digital optical densitometry (Scion Image Software, v.4.0.3.2, Scion, Frederick, MD, USA) and the values expressed in relation to the α-tubulin used as internal control.

Craniotomy and intravital microscopy

Intravital microscopy of brain microvasculature was performed, as described in Lacerda-Queiroz *et al*.(20), with slight modifications. In brief, on d 5 p.i., groups of 4–6 PbA-infected mice or NI animals, exposed or not to HBO, were anesthetized with ketamine (100 mg/kg) and xylazine (16 mg/kg) and maintained at 37°C using a heating pad. A skull opening of 3–4 mm diameter was made in the left parietal lobe using a surgical drill (Beltec, Araraquara, Brazil). Dura mater and arachnoid were lifted away from the skull to expose the pia mater blood vessels. To observe leukocyte/endothelium interactions, leukocytes were fluorescently labeled by intravenous administration of rhodamine 6G (0.3 mg/kg; MilliporeSigma) and observed using an Intravital Microscope (Axio ImagerA2; Carl Zeiss, Jena, Germany) with a ×10 objective and a 590 nm emission filter, coupled with a camera (AxioCam) to record images. The images obtained were analyzed using ImageJ software (NIH), and adhered leukocytes were counted. Adhered leukocytes were considered as those cells that remained attached for 30 s or more onto the endothelium. The counting of adherent leukocytes was expressed as cells attached to the endothelium in a 100-μm length of the vessel. Velocity (pixel/ms) of rhodamine 6G-labeled cells was determined using manual tracking plugin (ImageJ) in 3–4 movies for each condition. After the procedure, all animals were euthanized with a high dose of ketamine and xylazine.

Tissue processing

The presence of HIF-positive cells in the brain was considered evidence of tissue hypoxia. For this at a comparable time point, all mice were euthanized in an experiment when susceptible mice exhibited clinical signs of CM. PbA-infected mice demonstrated signs of CM at d 6–7 p.i., and most of these mice had entered the terminal phase of murine CM. On the day of euthanasia, groups of 4–6 PbA-infected mice or NI animals, exposed or not to HBO, were anesthetized with ketamine (100 mg/kg) and xylazine (16 mg/kg) and were perfused intracardially with phosphate-buffered 4% paraformaldehyde for 20 min. The brain was removed quickly, split sagittally, and immersion fixed in phosphate-buffered 4% paraformaldehyde for 2 h at room temperature before transfer to 70% ethanol. Tissues were processed for paraffin inclusion, which included immersion baths in ethanol-xylol-paraffin gradients. After inclusion, sections of 5 μm were obtained for immunohistochemical analysis.

Immunohistochemical analysis

The presence of HIF-1α-positive cells in brains of all mouse groups was detected by an immunohistochemical stain. Brain sections from midbrain were deparaffinized with xylene and hydrated in an ethanol gradient before staining. Directly after, incubation was performed with 1% H_2O_2 to block endogenous peroxidase activity (10 min). Henceforth, all procedures were done according to an ImmunoCruz rabbit ABC Staining System (sc-2018; Santa Cruz Biotechnology) datasheet. In brief, all sections were incubated with goat serum (MilliporeSigma) to avoid secondary antibody nonspecific binding for 1 h at room temperature and then incubated with specific primary antibodies to mouse HIF-1α (sc-10790; Santa Cruz Biotechnology) for 16 h at 4°C. After washing with saline phosphate buffer, sections were overlaid for 1 h with the biotin-conjugated secondary antibody at room temperature. This was followed by incubation with AB Enzyme reagent to amplification of the signal reaction. Bound antibodies were detected by reactivity with 3,3′-diaminobenzidine plus H_2O_2. After tap-water washing, the slides were counterstained by Harris Hematoxylin and mounted with Entellan. For immunohistochemical controls, primary antibodies were omitted from the staining procedure and were negative for any reactivity. Quantification of the immunostaining was done with ImageJ software. All slides were blinded and assessed using digital images. In total, 1000 cells were counted for each specimen using an ocular grid. The percentage of HIF-1α-positive cells was determined by a single observer (C.F.), blinded to the animal status, and defined as follows: percent of HIF-1α-positive cells = HIF-1α-positive cells/total cells.

Endothelial cell flow cytometry

Brains were removed from wild-type or Tie2cre HIF-1$\alpha^{fl/fl}$-infected mice (d 6 p.i.). Brains were digested with collagenase I for 30 min at 37°C. Cells (1–5 × 10^6) were incubated with FcBlock (BD Biosciences, San Jose, CA, USA), along with anti-F4/80 or anti-CD11b (Brilliant Violet 510), rat IgG1 isotope control or anti-CD31 (peridinin chlorophyll protein complex-cyanine 5.5), anti-CD54 (FITC), anti-CD142 (FITC), and anti-EPCR (phycoerythrin) for 30 min at 4°C in FACS buffer. Cells were then washed, resuspended in FACS buffer, and acquired using a BD LSR Fortessa cytometer (5 × 10^5 events/sample). Expression profiles in $CD31^+CD11b^-$ (endothelial cells) for ICAM-1 (CD54), tissue factor (CD142), and EPCR were then determined by the mean fluorescence intensity using FlowJo software (Ashland, OR, USA).

Total free heme quantification

Infected animals were anesthetized with ketamine (100 mg/kg) and xylazine (16 mg/kg), and blood samples were collected on d 6 p.i. from the vena cava using EDTA as an anticoagulant.

Thus, plasma was obtained after centrifugation at 1000 *g* for 15 min at 4°C for total free heme assessment. Total heme was quantified using a chromogenic assay, according to the manufacturer's instructions (QuantiChrom Heme Assay Kit; Bioassay Systems, Hayward, CA, USA).

Simultaneous Trp and kynurenine quantification

Trp and kynurenine (Kyn) concentrations in mouse serum were measured simultaneously by reverse-phase HPLC, as described in ref. 21, with some modifications. The HPLC system (Shimadzu, Kyoto, Japan) was coupled with an analytical octadecylsilyl C18 column of 15 cm, 4.6 μm, and a photodiode array detector (Shimadzu; collecting UV–visible spectra from 190 to 800 nm, which can provide chromatograms at the desired wavelength in this range). The mobile phase consisted a mixture of 15 mM sodium acetate buffer, with 27 ml acetonitrile adjusted to a final pH of 4 with acetic acid. Perchloric acid (final concentration 8%) was added to 200 μl mouse serum sample, homogenized by vortexing for 1 min, and centrifuged at 10,000 rpm at 4°C for 10 min. A clear supernatant was then injected into the HPLC system using an autosampler. In addition, Trp and Kyn HPLC grade reagents were purchased from MilliporeSigma, and stock solutions were prepared in mobile-phase buffer. For the standard curve, serial dilutions were used for Trp and Kyn (Trp/Kyn micromolars): 100/10, 50/5, 25/2.5, 12.5/1.25, 6.25/0.625, 3.125/0.325. The flow rate was 1.0 ml/min, and the volume per sample was 20 μl. Trp and Kyn were detected at 278 and 360 nm, respectively (22). Retention time was used to identify metabolites in the chromatogram, and standard curve was constructed by plotting the ratio of peak area (computed by LCsolution software; Shimadzu) of Trp or Kyn (*y* axis) against known Trp or Kyn concentration (*x* axis), respectively. The linearity of the standard curves was confirmed using regression variance analysis and significance of correlation coefficient, checked using Student's *t* test. A derived equation was used to quantify unknown concentrations in the mice samples. In addition, the intra-assay (reproducibility) variability was determined by analyzing samples in triplicate and the interassay (repeatability) variability by testing samples, 3 and 6 d in triplicate after the first analysis. The concentration compared in inter- and intra-assay had no statistically significant difference.

Statistical analysis

Statistical significance was determined using 1-way ANOVA or Student's *t* test for parametric data. Kruskal-Wallis and *post hoc* or Mann-Whitney *U* tests were used for nonparametric data. Mantel-Cox test was used for comparison of survival curves. All statistical analyses were performed using BioEstat v.5.0 (CNPq, Brasília, Brazil) and Prism v.5.0 (GraphPad Software, La Jolla, CA, USA). Values were considered significant when $P < 0.05$.

RESULTS

HBO treatment decreases parasite and leukocyte accumulation in the brain of mice during PbA infection

We have shown that HBO protects mice against ECM by reducing expression of proinflammatory cytokines and sequestration of T cells in the brain of PbA-infected mice, which in turn, prevent BBB disruption and delay CM-specific neurologic signs (18). In addition to sequestration of $CD8^+$ T cells in the CNS, the concomitant presence of parasitized erythrocytes is thought to be crucial for CM development (23). Thus, we asked whether pressurized oxygen would modulate the parasite load in the brain. To this end, qRT-PCR for PbA 18S rRNA was performed on material extracted from the brains of PbA-infected mice untreated (PbA) and HBO treated (PbA-HBO), either before or after intracardiac perfusion. There was no significant difference in parasite 18S rRNA in the brain of infected animals before intracardiac perfusion (**Fig. 1*A***). However, parasite 18S rRNA was significantly lower ($P = 0.0079$) in the brain of PbA-HBO mice compared with PbA mice after intracardiac perfusion at d 6 p.i. (Fig. 1*B*).

Cerebral blood flow impairment by adherent leukocytes and parasites is a common feature in CM (6–8). Therefore, we also assessed whether HBO would affect leukocyte interaction with brain endothelium by intravital microscopy of PbA-infected mice. Representative intracranial photomicrographs for each tested group are shown (Fig. 1*C, D*), and movies of NI animals—PbA-infected mice, exposed or not to HBO—were recorded at real-time conditions (Supplemental Movies S1–3). In sharp contrast to PbA mice, exposure to HBO significantly inhibited leukocyte adhesion to the brain microvasculature ($P < 0.0001$; Fig. 1*C*) and significantly improved microcirculation velocity (Fig. 1*D*).

HBO treatment also resulted in reduction of mRNA expression of *Lfa1* and perforin, by 50 and 70%, respectively, in the brain of PbA mice (Fig. 1*E, F*). As these molecules are closely related to adhesion and function of effector leukocytes cells, these observations support our hypothesis that HBO treatment decreases leukocyte adhesion in the brain microvasculature.

To address whether decreased leukocyte adhesion to brain endothelial cells in PbA-HBO mice was a result of decreased activation of leukocytes from the periphery, we analyzed mRNA expression of different integrins—*itga1*, *itgb1*, and *itgb2* (components of the LFA-1 protein complex)—molecules expressed in activated leukocytes. Surprisingly, in total peripheral leukocytes (peripheral blood or spleen derived), mRNA expression of all integrins analyzed was similar in PbA-HBO and PbA control mice (**Fig. 2**). Furthermore, only mRNA expression of *itga1* in leukocytes from blood and *itgb1* in leukocytes from spleen was increased after HBO treatment (Fig. 2). Taken together, these observations indicate that the protective effect of HBO treatment during ECM is not related to a direct immunosuppressive effect on immune cells. Instead, our data point to the fact that HBO may be targeting activation of the brain endothelial cells during ECM.

HBO treatment decreases activation of brain endothelial cells during PbA infection

It is known that brain endothelial cell activation is one of the hallmarks of ECM development (23–27), and our

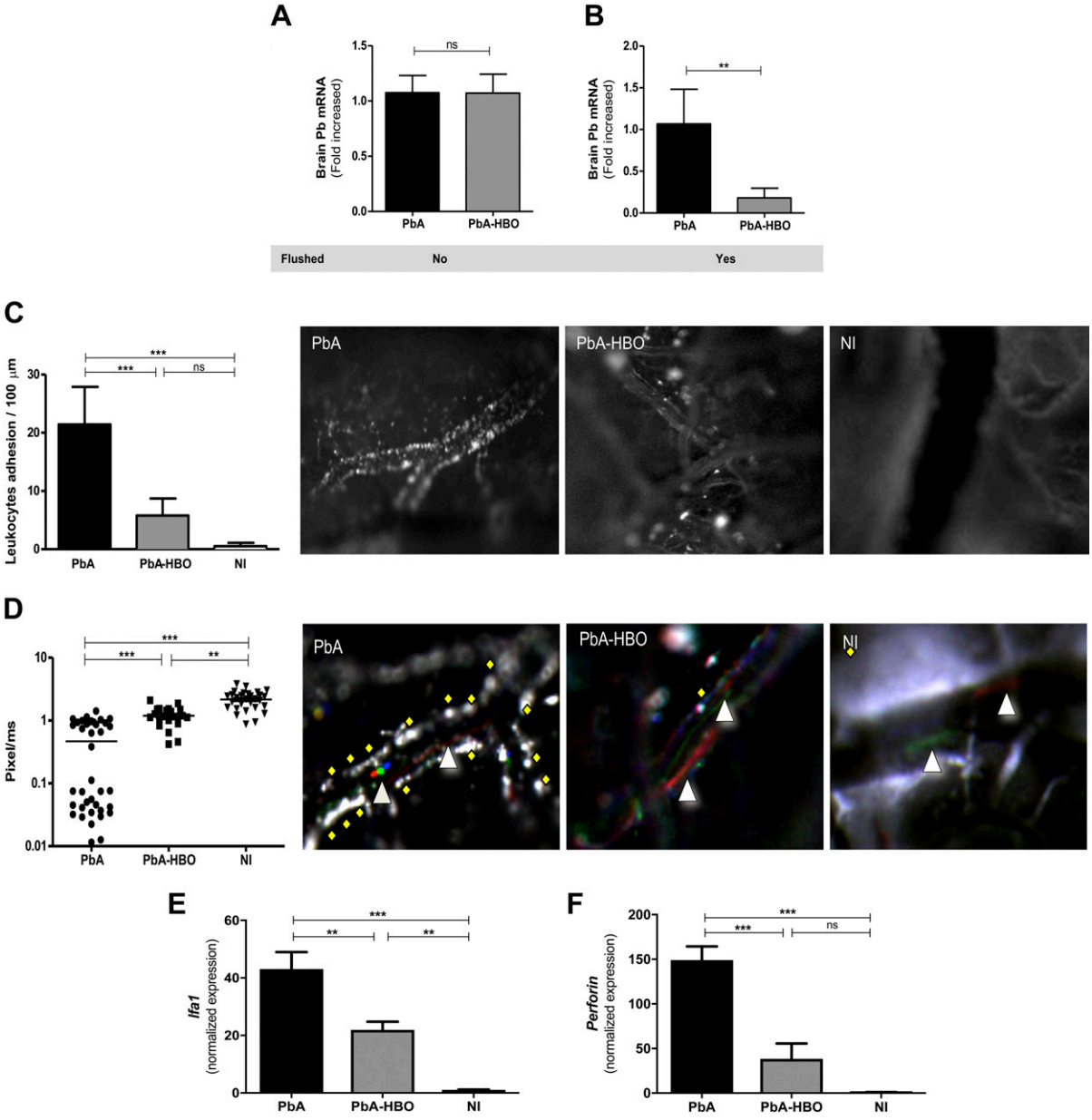

Figure 1. HBO reduces parasite and leukocyte accumulation in the brain of infected mice after intracardiac perfusion. Mice infected with PbA (PbA group) were exposed daily, or not, to HBO (PbA-HBO) conditions (100% O_2, 3 ATA, 1 h). *A*, *B*) On d 6–7 p.i., when mice showed signs of ECM, brains were collected in nonflushed (*A*) or flushed (*B*) animals, and *P. berghei* 18S rRNA levels were quantified by qRT-PCR. Values represent the means of specific 18S gene expression normalized to HPRT ± SD. $^{**}P < 0.01$ (Student's *t* test). *C*, *D*) With the use of intravital microscopy, leukocyte adhesion to brain microvasculature and microcirculation velocity of groups of 4–6 mice, NI or infected with PbA and exposed to HBO (PbA-HBO) or not HBO-treated (PbA) were assessed on d 5 p.i. Results are expressed as the means of adhered leukocytes per 100 µm in at least 4 vessels ± SD. $^{**}P < 0.01$, $^{***}P < 0.001$ (ANOVA test). Representative brain microcirculation photomicrographs of NI, PbA, and PbA-HBO mice show leukocyte adhesion (*C*) and microcirculation flow velocity (*D*) of rhodamine 6G-labeled cells. The triangles indicate cells with high speed, diamonds represent cells with low speed that drag on the endothelium, and the red dots represent the mean velocities of labeled cells. *E*, *F*) On d 6–7 p.i., when mice showed signs of ECM, brains were collected and *Lfa1* and *Perforin* levels were quantified by qRT-PCR. Results were normalized to HPRT, and means ± SD of biologic triplicates are shown compared with NI mice. Ns, nonsignificant, $^{**}P < 0.01$, $^{***}P < 0.001$ (ANOVA test).

results indicate that HBO-protective effects could involve inhibition of brain endothelial cell activation during ECM. Therefore, to examine if indeed this is a potential HBO-induced mechanism leading to reduced parasite and leukocyte accumulation in the brain of PbA-infected mice, we assessed mRNA expression of molecules associated with endothelial cell activation in mouse brains during ECM. PbA-HBO mice had significantly lower mRNA levels of *Icam1* (**Fig. 3*A***) and *Epcr* (Fig. 3*B*; $P < 0.05$ and $P < 0.01$, respectively) when compared with PbA mice, whereas *tissue factor* (CD142) expression was not changed in any group (Fig. 3*C*). This result supports our hypothesis that HBO affects endothelial cell activation during ECM.

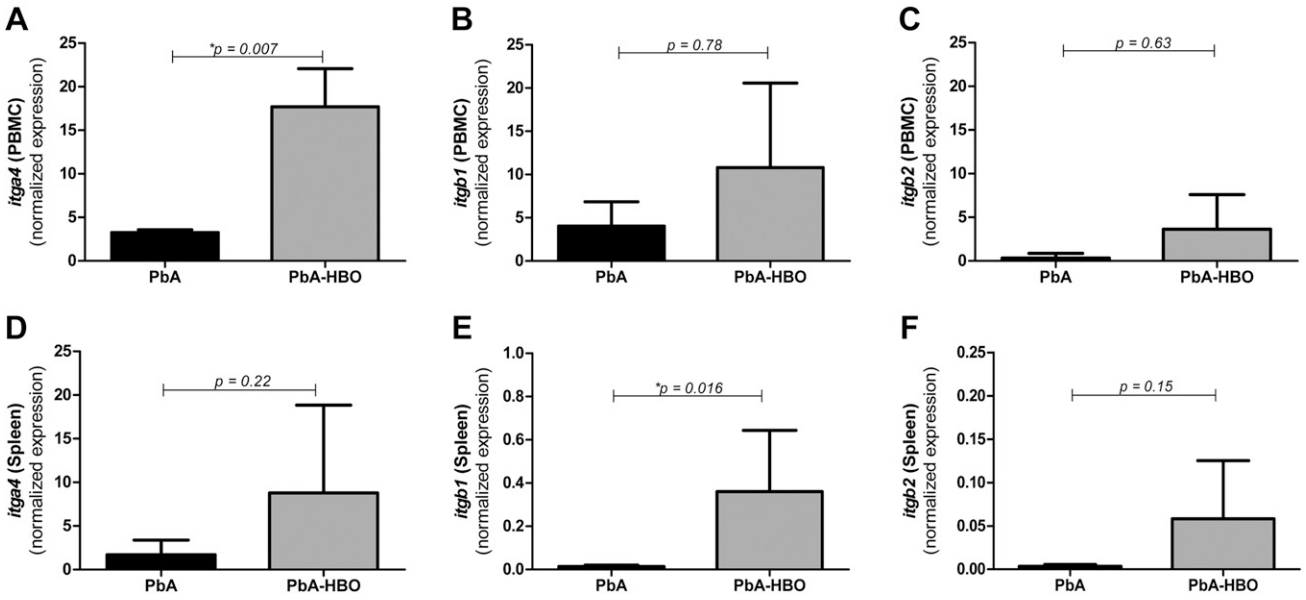

Figure 2. Genetic expression of integrins in peripheral blood- or spleen-derived leukocytes. Groups of 5–7 animals infected with 10^6 PbA iEs (PbA group) were daily exposed, or not, to HBO (PbA-HBO) conditions (100% O_2, 3 ATA, 1 h). On d 6–7 p.i., when PbA mice showed signs of ECM, leukocytes were isolated from the peripheral blood [peripheral blood mononuclear cells (PBMCs)] (*A–C*) or from the spleen and *itga4*: ITGA4 (*D*); *itgb1*: ITGB1 (*E*); and *itgb2*: ITGB2 (*F*) levels were assessed by qRT-PCR. Results were normalized to HPRT, and means and SD of biologic triplicates are shown compared with NI mice. $^*P < 0.05$.

HBO treatment decreases cerebral hypoxia induced by PbA infection

It has been demonstrated in postmortem studies in CM patients and murine models of CM that some of the deleterious consequences of leukocyte and parasite accumulation in the activated endothelium of the host brain vessels are vascular obstructions and impairment of tissue perfusion (28). Impairments of cerebral microcirculatory blood flow caused an ischemic process leading to cerebral hypoxia (10, 28, 29), which was associated with endothelial activation and BBB disruption, resulting in an increased permeability, subsequent edema, and tissue damage (29–31). Therefore, hypoxia is also a key event in development of acute cerebral disease (29, 30). Importantly, during the hypoxia-associated response, the transcription factor HIF-1α is rapidly upregulated, and its transcriptional program is activated in different cell types, including endothelial cells (32, 33). Thus, because we observed a lower parasite and leukocyte accumulation, as well as lower endothelial cell activation in the brain microvasculature after HBO treatment, we investigated whether exposure to HBO also reduced the hypoxic response in the brains of PbA mice. As shown in **Fig. 4*A***, few areas and cells are HIF-1α^+ in NI mice. However, the levels of HIF-1α^+ cells were significantly increased in PbA mice when compared with PbA-HBO animals (Fig. 4*A*). To regulate gene expression, HIF-1α requires its binding partner, the Ahr nuclear translocator (ARNT). ARNT is also required by the AhR, a crucial regulator that mediates many of the responses to toxic environmental chemicals (34). It has been shown that HIF-1α and AhR compete for binding to ARNT, thus establishing a crosstalk between hypoxia- and AhR-induced gene-expression profiles (34). Moreover, HIF-1α induction promotes AhR ubiquitination and proteasomal degradation (35). Accordingly, here we observed a lower AhR protein expression in the brains of PbA mice, whereas HBO treatment prevented downregulation of AhR expression (Fig. 4*B*).

It has been shown that HIF-1α transcriptional activity results in upregulation of HO-1 expression (36, 37). In addition, HO-1 is induced by the release of free heme in the plasma as a result of parasite growth (38, 39). We assessed *Hmox1* expression to verify whether ECM-induced tissue hypoxia increases transcriptional activity of HIF-1α and if HBO inhibits this process. Accordingly, Fig. 4*C* shows upregulation of *Hmox1* expression in the brain of PbA-infected mice, whereas *Hmox1* was significantly reduced (2-fold; $P < 0.0001$) in the brain of PbA-HBO mice at d 6–7 p.i. This set of results shows that HBO treatment resulted in reduction of hypoxia-associated HIF-1α transcriptional activity in the brains of PbA-infected mice.

However, the observation that HBO strikingly reduces expression of *Hmox1* and modestly reduces expression of HIF-1α raises the possibility that HBO could downregulate HO-1 expression by another mechanism. HO-1 is also induced by free heme (40). Here and previously (18), we showed that HBO therapy resulted in a significantly reduced parasite burden in the brain of PbA-infected mice, which could decrease the release of free heme into the plasma. Accordingly, here, we observed that administration of pressurized oxygen in PbA-infected mice significantly reduced total heme levels on d 5 and 6 p.i., when ECM clinical signs begin to appear (Fig. 4*D*). Thus, HBO treatment downregulates HO-1 expression in brains of infected mice by both reducing hypoxia and by slowing parasite growth and the release of free heme into the plasma. Taken together, these results show that the

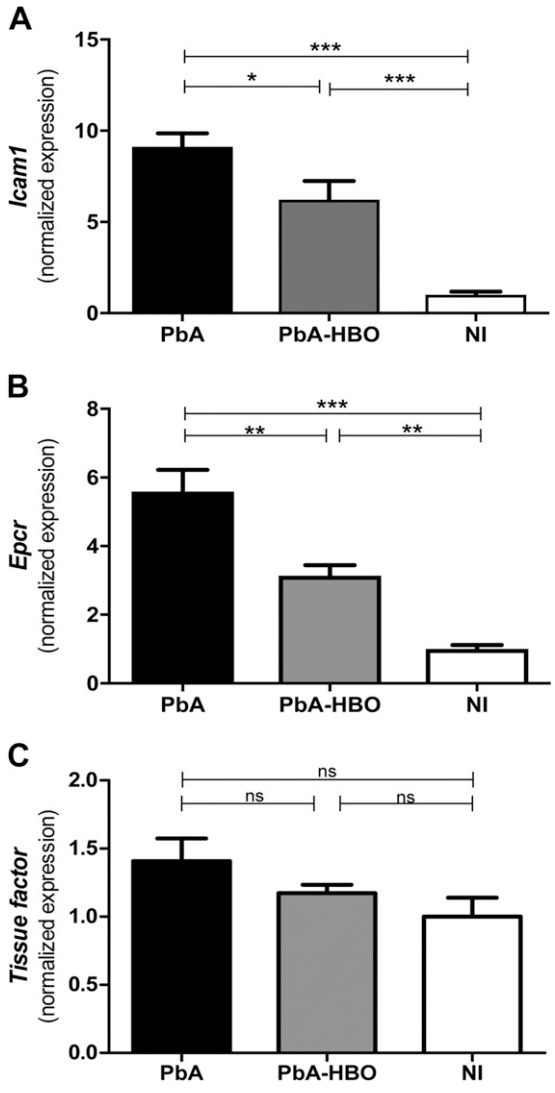

Figure 3. HBO reduces endothelial activation in the brain of infected animals. Total brain mRNA from PbA-infected mice or PbA mice exposed to HBO (PbA-HBO) was submitted to qRT-PCR for *Icam1*(*A*), *Epcr* (*B*), and *tissue factor* (*C*) genes. Results were normalized to HPRT, and means ± SD of biologic triplicates are shown compared with NI mice. $^{*}P < 0.05$, $^{**}P < 0.01$, $^{***}P < 0.001$ (ANOVA test).

hypoxia-triggered response during PbA infection is inhibited by HBO treatment.

Lack of HIF-1α expression in endothelial cells is protective against ECM

Our results indicate that endothelial cells are an important target of HBO-induced protective molecular mechanisms during ECM, probably by downregulation of the proinflammatory hypoxic response (10, 29). Thus, to address whether during ECM, HBO inhibits the hypoxia-triggered response in brain endothelial cells through inhibition of HIF-1α-dependent transcriptional activity, we created a Tie2cre HIF-1$\alpha^{fl/fl}$ mouse strain that lacked HIF-1α in endothelial cells (19). As *Ahr* mRNA and *Hmox1* expression is regulated by HIF-1α-induced transcriptional activity, we tested whether HIF-1α deletion in brain endothelial cells would affect expression of both genes during infection with PbA. Similar to PbA-HBO mice, **Fig. 5*A*** shows that *Ahr* gene expression was significantly higher, whereas *Hmox1* expression was lower in the absence of endothelial cell HIF-1α (Fig. 5*B*). These results indicate that the PbA-induced hypoxic response, represented by the decrease of *AhR* expression and increase of *Hmox1* expression, was abrogated in the absence of HIF-1α in the brain endothelial cells. Furthermore, in the brains of PbA-infected Tie2cre HIF-1$\alpha^{fl/fl}$ mice, we found lower mRNA levels of the proinflammatory cytokine IL-12, also a target of HIF-1α transcriptional activity and associated with murine CM pathogenesis (41) (Fig. 5*C, D*). Although we did not observe changes in ICAM-1 and EPCR protein expression (data now shown), we verified lower tissue factor (CD142) expression in brain-derived endothelial cells from the Tie2cre HIF-1$\alpha^{fl/fl}$ gene during PbA infection (Fig. 5*E*). These observations indicate that brain endothelial cell activation is, in part, induced by the HIF-1α-mediated proinflammatory hypoxic response during ECM, as previously described in hypoxic-ischemic conditions in Kaur *et al*. 30. Consistent with our hypothesis that the ECM-protective activity of HBO occurs by dampening an HIF-1α-mediated hypoxic proinflammatory response, Tie2cre HIF-1$\alpha^{fl/fl}$ mice were resistant to development of ECM and showed a survival rate similar to that of PbA-HBO mice (Fig. 5*F*) (18).

HBO treatment inhibits Kyn pathway of Trp metabolism

Our results show that the balance between the response to hypoxia mediated by HIF-1α and AhR expression might play a critical role during CM pathogenesis.

Several endogenous ligands have been identified to bind, activate, and decrease AhR expression following ligand binding, for instance, Kyn, a product of the IDO-1-dependent Trp metabolism through the Kyn pathway (KP) (34, 42, 43). IDO-1, which catalyzes the initial and rate-limiting step of this pathway, is upregulated by IFN-γ in the cerebral microvascular endothelium in *Plasmodium*-infected mice with CM (44). Kyn levels, the first breakdown product of the KP, increase in the plasma and accumulate in the cerebral blood vessels of mice infected with PbA, reaching concentrations in the high micromolar to low millimolar range (45). In addition, a decrease of Trp levels and an increase in the Kyn:Trp ratio have been described in several pathologies associated with chronic immune activation, including malaria, implicating activation of the KP in CM pathogenesis (42, 44, 46). In this regard, because HBO seems to restore the balance toward increased AhR expression, as observed in physiologic conditions, we evaluated if HBO treatment could also affect the expression of some key components of the KP. We verified that *Ido1* mRNA expression is upregulated in the brain of PbA-infected mice. Kyn levels and the Kyn:Trp ratio in the serum of PbA mice were increased, whereas Trp levels did not change (**Fig. 6**). Importantly, HBO treatment

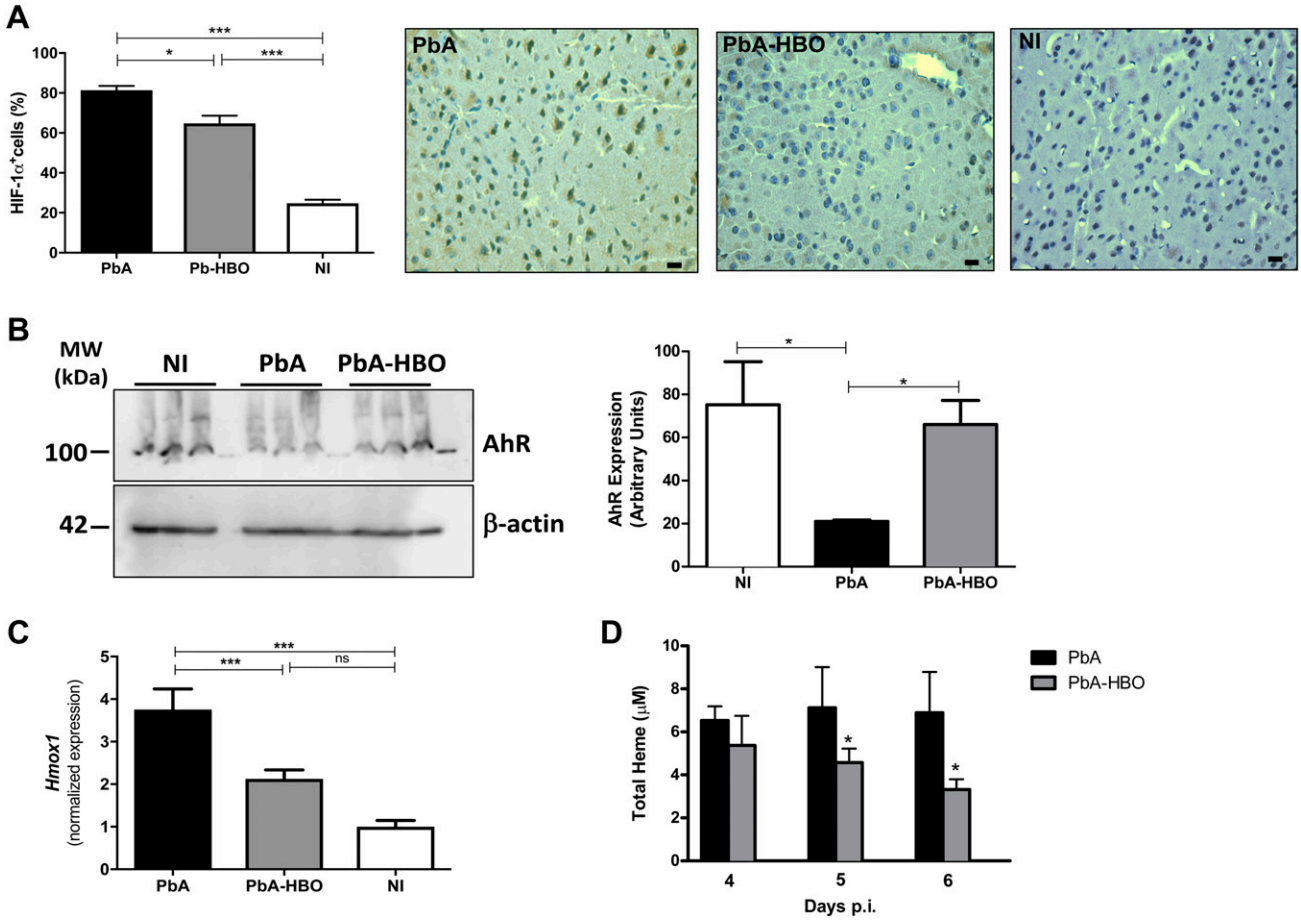

Figure 4. HBO reduces hypoxia in the brain of infected animals. *A*) Representative images of HIF-1α$^+$ cells in brains of NI, PbA, and PbA-HBO mice. Values represent means ± SD of 6 mice per group and are representative of 2 independent experiments with similar results. *$P < 0.05$, ***$P < 0.001$ (ANOVA test). *B*) On d 6–7 p.i., brains were collected and AhR expression was assessed by Western blot. Values represent means ± SD of 6 mice per group and are representative of 2 independent experiments with similar results. *$P < 0.05$ (ANOVA test). *C*) *Hmox1* brain expression levels in PbA and PbA-HBO mice were determined by qRT-PCR. Results were normalized to HPRT, and means and SD of biologic triplicates are shown compared with NI mice. ***$P < 0.001$ (ANOVA test). *D*) Quantification of free heme was determined, at d 4–6 in the plasma of infected mice exposed, or not, to HBO. The results represent the average of 6–8 animals per group ± SD. *$P < 0.05$ (ANOVA test).

inhibited upregulation of *Ido1* expression and reduced Kyn production and the Kyn:Trp ratio in the infected mice (Fig. 6), indicating that HBO inhibits PbA-induced Kyn production and probably the generation of downstream neurotoxic metabolites (41, 42).

DISCUSSION

Previously, we demonstrated a neuroprotective effect of HBO during ECM (18). In the present study, our goal was to provide an understanding of the protective molecular mechanisms of pressurized oxygen in PbA-infected animals. Our results here show that HBO treatment reduced parasite and leukocyte accumulation in the brain by targeting the activation of brain microvascular endothelial cells. In addition, HBO treatment prevented an hypoxia-mediated proinflammatory response, as demonstrated by decreased HIF-1α expression and transcriptional activity, while stabilizing AhR expression in the brain of PbA mice. The biologic significance of such effects was confirmed in mice lacking HIF-1α in endothelial cells (Tie2cre HIF-1α$^{fl/fl}$), which were resistant to ECM.

It is important to consider which aspects of this model fit better with human CM. It has been demonstrated in the murine model that parasite accumulation in the brain microvasculature activates endothelial cells through release of inflammatory ligands, such as glycosylphosphatidylinositol anchors and hemozoin crystals bound to parasite DNA (31). In turn, activated brain endothelial cells respond to these stimuli by upregulating adhesion receptors and molecules involved in antigen presentation and secreting chemokines and cytokines. Consequently, leukocytes and platelets are recruited and activated, feeding a local proinflammatory cycle by promoting more endothelial activation, leukocyte/platelet sequestration, and parasite accumulation (24, 47). Moreover, activated CD8$^+$ T cells migrate toward the chemokine gradient to the brain, and LFA-1 promotes their adhesion to endothelial ICAM-1. Furthermore, locally secreted proinflammatory cytokines stimulate brain endothelial cells to phagocytose and cross present

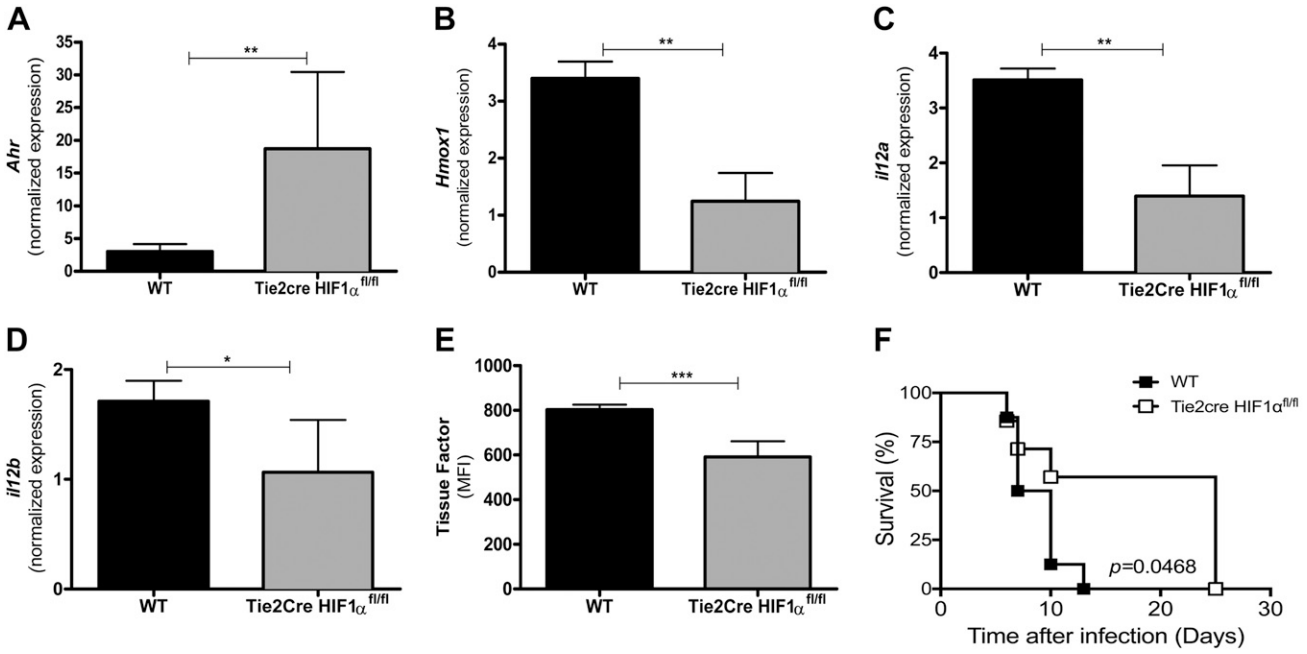

Figure 5. Lack of HIF-1α expression in endothelial cells is protective against ECM. *A–D*) Groups of 10–15 wild-type (WT) or Tie2cre HIF-1α$^{fl/fl}$ mice lacking HIF-1α in endothelial cells were infected with 10^6 PbA-iEs. On d 6–7 p.i., *Ahr* (*A*), *Hmox* (*B*), *il12a* (*C*), and *il12b* (*D*) levels were assessed by qRT-PCR. As controls, brains of NI mice were used. Values were expressed as the means of specific *Ahr*-, *Hmox*-, *il12a*-, or *il12b*-normalized expression of 10 mice ± SD. $^{**}P < 0.01$, $^{*}P < 0.05$ (ANOVA test). *E*) Tissue factor protein expression was determined by the mean fluorescence intensity (MFI) in CD31$^+$CD11b$^-$ (endothelial cells). The results represent the average of 10 animals per group ± SD. $^{***}P < 0.001$ (ANOVA test). *F*) Survival of the indicated PbA-infected mouse strains.

parasite-derived epitopes to CD8$^+$ T cells. In turn, CD8$^+$ T cells secrete perforin and granzymes, which disrupt the BBB (24, 47). In regard to human CM, a study conducted with >100 isolates collected from *P. falciparum*-infected individuals demonstrated an association between endothelial cell activation and CM (14). Moreover, different studies show that ICAM-1 and EPCR are upregulated in the brain endothelium of CM patients and are implicated in parasite accumulation (13, 14, 47). Importantly, in a systematic postmortem study of the brains of Malawian children with CM, few CD8$^+$ T cells were observed intravascularly in distended capillaries (48). This is similar to mice infected with PbA, where the relatively small numbers of sequestered CD8$^+$ T cells are diffcult to observe by

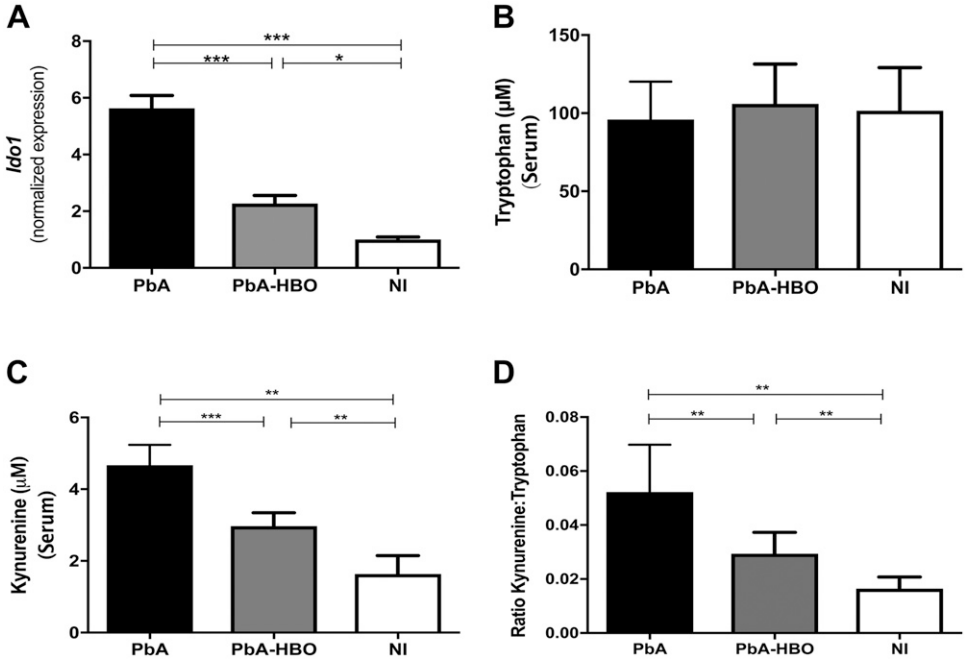

Figure 6. HBO treatment inhibits the KP of the Trp metabolism. *A*) *Ido1* mRNA brain expression levels from PbA-iE or PbA-HBO mouse groups were determined by qRT-PCR. The NI mouse group was used as control. $^{*}P < 0.05$, $^{***}P < 0.001$ (ANOVA test). *B–D*) Concentration of Trp (*B*), Kyn (μm) (*C*), and Kyn:Trp (*D*) ratio were determined in the serum of the different mouse groups. Values represent means ± SD of 7 mice per group and are representative of 2 independent experiments with similar results. $^{**}P < 0.01$, $^{***}P < 0.001$ (ANOVA test).

histology (49), which do not exclude the possibility that $CD8^+$ T cells play an important role in human CM pathogenesis. In this context, we have shown that HBO treatment reduces the expression of proinflammatory cytokines and sequestration of $CD4^+$ and $CD8^+$ T cells in the brain of PbA mice, which in turn, prevent BBB disruption and delay CM-specific neurologic signs (18). Here, we also verified that HBO significantly reduces parasite and leukocyte accumulation in the brain microvasculature by inhibiting endothelial cell activation, which improved microcirculation velocity. Interestingly, even though leukocyte activation is not modulated by pressurized oxygen, as demonstrated by the expression of *ItgaI*, *Itgab1*, and *Itgab2* in cells isolated from the peripheral blood or the spleen, expression of LFA-1 and perforin in the brain of PbA-HBO mice was significantly decreased compared with control mice. These data suggest that HBO treatment did not target immune cells, but instead, it may target brain endothelial cells affecting their capacity to promote leukocyte sequestration.

It has also been demonstrated in postmortem studies in CM patients and murine models of CM that parasite and leukocyte accumulation, associated to endothelial cell activation, increases vascular resistance and promotes obstructions, thereby contributing to impaired cerebral perfusion during CM. These impairments of cerebral microcirculatory blood flow are thought to cause ischemia and cerebral hypoxia. The microvascular hemodynamics and oxygenation are drastically compromised during ECM, resulting in lower O_2 delivery and O_2 extraction by the brain tissue (28, 29). To maintain normal brain function and cell survival, oxygen-sensing mechanisms operate at the cellular level in response to hypoxia. In particular, the transcription factor HIF-1α plays a central role in hypoxia sensing. In the brain, HIF-1α expression is induced by hypoxia in neurons, astrocytes, ependymal cells, and endothelial cells (33, 34). Under normal conditions, the oxygen-regulated HIF-1α subunit is rapidly degraded *via* prolyl hydroxylation that targets its degradation in the proteasome. Hypoxia inhibits prolyl hydroxylase activity, resulting in HIF-1α subunit stabilization in the cytoplasm and translocation to the nucleus, where it dimerizes with ARNT to form HIF-1. HIF-1 then binds to hypoxia-responsive elements in promotor regions of target genes involved in cellular adaptation to hypoxic stress and induces their expression (33, 34). However, HIF-1α signaling could be deleterious in some circumstances by inducing expression of proapoptotic proteins of the B cell lymphoma 2 family, leading to cell death (33, 34). Hypoxia could also induce BBB dysfunction through increased tyrosine phosphorylation and redistribution of tight junction proteins away from cell borders and VEGF secretion (31). Conversely, inhibition of HIF-1 improves barrier function in hypoxic cells, indicating that temporal suppression of HIF-1 activity may be essential to preserve barrier function during injury (31). In addition, we cannot rule out that other factors, including cytokines, such as IFN-γ, IL-1β, or TNF and NF-κB, may play a more direct role in inducing HIF-1α, regardless of the oxygen levels (41, 50). In turn, hypoxia also triggers a proinflammatory response that can activate endothelial cells (30). Furthermore, the biologic relevance of such HBO effects, particularly those targeting endothelial cells, was unequivocally demonstrated in PbA-infected mice lacking HIF-1α expression in endothelial cells (Tie2cre HIF-$1\alpha^{fl/fl}$), which showed a comparable level of survival improvement and protection against CM with that observed in PbA-HBO mice. Thus, reduction of the proinflammatory hypoxic response, resulting from HBO treatment, may explain the protective effects observed in PbA-HBO mice (18).

It is known that there is a crosstalk between hypoxia and AhR signaling pathways, as both require ARNT as a binding partner (33, 34). In addition, HIF-1α activity promotes AhR ubiquitination and proteasomal degradation (35). This interaction has been described in human cerebral microvascular endothelial cells, indicating that it could play a role in cellular responses after reduced oxygen availability at the BBB (51). In this regard, AhR plays a protective role during ECM. There is a significant downregulation of AhR expression in the brain during PbA infection, and AhR-deficient mice are highly susceptible to PbA infection (52). These mice display increased parasitemia, earlier mortality, enhanced leukocyte sequestration, and increased inflammation in the brain (52). Thus, AhR-protective effects seem to involve control of parasite replication and induction of immune responses required for host resistance, probably *via* activation of suppressor of cytokine signaling 1 and 3 pathways (52). Accordingly, here, we observed reduced AhR expression in brain endothelial cells of PbA-infected mice, whereas HBO treatment prevented downregulation of AhR expression. Together, our data show an inverse correlation of HIF-1α and AhR expression during ECM, indicating that the predominant orchestration of HIF-1α or AhR signaling pathways in the brain could determine a better or worse malaria outcome.

Significant alterations of the Trp metabolism have been described in different pathologic conditions related to immune activation and inflammation, such as infections, including malaria, autoimmune syndromes, various types of cancer, cardiovascular disease, and neurodegenerative processes (44, 46). A decrease of Trp concentration, along with an elevated Kyn:Trp ratio in plasma, cerebrospinal fluid (CSF), and other body fluids, is common in these conditions (44, 46). In addition, evidence shows that the IDO-dependent Trp degradation through the KP is involved in CM pathogenesis (42, 44, 46). Quinolinic acid (QA) levels, a metabolite downstream of the KP and associated with glutamate receptor-mediated excitotoxicity and impairment of BBB integrity, are elevated during CM (44). Furthermore, the concentration of Kyn acid (KA), an upstream metabolite of KP, thought to be neuroprotective, is decreased (44). These findings suggest that the Trp metabolism, through the KP, could be relevant to the hyperexcitability observed in murine and human CM. Accordingly, with the findings in murine models, Kenyan children with CM had a 14-fold greater concentration of QA in their CSF compared with an age-matched control set (44). Elevated QA was also found in CSF of Malawian

children with CM associated with a clinical history of convulsions (44). In Vietnamese adults, the QA level in the CSF and QA:KA ratio was significantly elevated, although this might have been a consequence of renal failure in these patients (44). At the cellular level, endothelial cells at the BBB and pericytes constitutively express components of the KP and synthesize Kyn and KA, which are secreted basolaterally (46, 53). The secreted Kyn can be further metabolized by perivascular macrophages and microglia with synthesis of QA (53). This could explain why KP activation at the BBB could result in local neurotoxicity, pointing to a mechanism whereby a systemic inflammatory signal can be transduced across an intact BBB to cause local neurotoxicity. However, despite the fact that the KP is highly active in the periphery, only Trp, Kyn, and 3-hydroxy-*l*-Kyn can be transported through the BBB to serve as substrates for production of neurotoxic metabolites in the CNS (54). Thus, another potential molecular mechanism of protection induced by HBO treatment during CM could be a result of the overall decrease in the availability of Kyn in the periphery and CNS that might subsequently affect the generation of neurotoxic metabolites derived from Trp degradation through the KP. Future in-depth studies are needed to ascertain the impact of HBO treatment on Trp catabolism in the CNS.

In summary, our data show, for the first time, the neuroprotective molecular pathways induced by HBO treatment during ECM. These insights support its potential as a supportive therapy in association with conventional treatment to improve poor CM outcomes. In addition, our data provide a molecular basis for the use of HBO in therapeutic strategies to improve treatment outcomes of other disorders affecting the brain. FJ

ACKNOWLEDGMENTS

This work was supported by Fundação de Amparo à Pesquisa do Estado de São Paulo (FAPESP) Grants 2012/16525-2 (to F.T.M.C.), 2014/20451-0 (to S.E.), 2016/07030-0 (to C.R.F.M.), and 2016/12855-9 (to J.L.S-F.); FAPESP (*http://www.fapesp.br/en/*); and U.S. National Institutes of Health, National Institute of Allergy and Infectious Diseases Grant AI118302-02. A.S.F., C.C.W., S.G., L.V., S.E., C.R.F.M., and F.T.M.C. are Conselho Nacional do Desenvolvimento Científico e Tecnológico (CNPq) research fellows. The funders had no role in study design, data collection and analysis, decision to publish, or preparation of the manuscript. The authors declare no conflicts of interest.

AUTHOR CONTRIBUTIONS

M. F. Bastos, A. C. A. V. Kayano, N. Shryock, J. Aliberti, and F. T. M. Costa designed research; M. F. Bastos, A. C. A. V. Kayano, Y.C. Blanco, C. Judice, J. L. Silva-Filho, J. C. K. Dos-Santos, N. Shryock, M. K. Sercundes, L. S. Ortolan, C. Francelin, J. A. Leite, R. M. Elias, R. Oliveira, N. O. S. Câmara, S. C. P. Lopes, L. Albrecht, A. S. Farias, and C. P. Vicente analyzed data; R. M. Elias, N. O. S. Câmara, C. C. Werneck, S. Giorgio, L. Verinaud, S. Epiphanio, C. R. F. Marinho, P. Lalwani, R. Amino, J. Aliberti, and F. T. M. Costa performed research; J. L. Silva-Filho, M. F. Bastos, A. C. A. V. Kayano, J. C. K. Dos-Santos and C. Judice wrote the paper; C.C. Werneck, S. Giorgio, L. Verinaud, S. Epiphanio, C. R. F. Marinho, P. Lalwani, R. Amino, J. Aliberti and F. T. M. Costa contributed new reagents or analytic tools; M. F. Bastos, A. C. A. V. Kayano, Y.C. Blanco, J. C. K. Dos-Santos, C. Judice, J. A. Leite, M. K. Sercundes, L. S. Ortolan, C. Francelin, R. M. Elias, N. O. S. Câmara, N. Shryock, J. Aliberti, and F. T. M. Costa performed and recorded experiments; and N. Shryock and J. Aliberti performed all experiments with Tie2cre HIF-1a$^{fl/fl}$ mice.

REFERENCES

1. World Health Organization. (2015) *World Malaria Report 2015*, World Health Organization, Geneva, Switzerland
2. Idro, R., Jenkins, N. E., and Newton, C. R. (2005) Pathogenesis, clinical features, and neurological outcome of cerebral malaria. *Lancet Neurol.* **4**, 827–840
3. Dondorp, A. M., Fanello, C. I., Hendriksen, I. C., Gomes, E., Seni, A., Chhaganlal, K. D., Bojang, K., Olaosebikan, R., Anunobi, N., Maitland, K., Kivaya, E., Agbenyega, T., Nguah, S. B., Evans, J., Gesase, S., Kahabuka, C., Mtove, G., Nadjm, B., Deen, J., Mwanga-Amumpaire, J., Nansumba, M., Karema, C., Umulisa, N., Uwimana, A., Mokuolu, O. A., Adedoyin, O. T., Johnson, W. B., Tshefu, A. K., Onyamboko, M. A., Sakulthaew, T., Ngum, W. P., Silamut, K., Stepniewska, K., Woodrow, C. J., Bethell, D., Wills, B., Oneko, M., Peto, T. E., von Seidlein, L., Day, N. P., and White, N. J.; AQUAMAT group. (2010) Artesunate versus quinine in the treatment of severe falciparum malaria in African children (AQUAMAT): an open-label, randomised trial. *Lancet* **376**, 1647–1657; erratum, (2011) **377**, 126
4. John, C. C., Bangirana, P., Byarugaba, J., Opoka, R. O., Idro, R., Jurek, A. M., Wu, B., and Boivin, M. J. (2008) Cerebral malaria in children is associated with long-term cognitive impairment. *Pediatrics* **122**, e92–e99
5. John, C. C., Panoskaltsis-Mortari, A., Opoka, R. O., Park, G. S., Orchard, P. J., Jurek, A. M., Idro, R., Byarugaba, J., and Boivin, M. J. (2008) Cerebrospinal fluid cytokine levels and cognitive impairment in cerebral malaria. *Am. J. Trop. Med. Hyg.* **78**, 198–205
6. Dondorp, A. M., Omodeo-Salè, F., Chotivanich, K., Taramelli, D., and White, N. J. (2003) Oxidative stress and rheology in severe malaria. *Redox Rep.* **8**, 292–294
7. Van der Heyde, H. C., Nolan, J., Combes, V., Gramaglia, I., and Grau, G. E. (2006) A unified hypothesis for the genesis of cerebral malaria: sequestration, inflammation and hemostasis leading to microcirculatory dysfunction. *Trends Parasitol.* **22**, 503–508
8. Francischetti, I. M., Seydel, K. B., and Monteiro, R. Q. (2008) Blood coagulation, inflammation, and malaria. *Microcirculation* **15**, 81–107
9. Seixas, E., Gozzelino, R., Chora, A., Ferreira, A., Silva, G., Larsen, R., Rebelo, S., Penido, C., Smith, N. R., Coutinho, A., and Soares, M. P. (2009) Heme oxygenase-1 affords protection against noncerebral forms of severe malaria. *Proc. Natl. Acad. Sci. USA* **106**, 15837–15842
10. Hunt, N. H., and Grau, G. E. (2003) Cytokines: accelerators and brakes in the pathogenesis of cerebral malaria. *Trends Immunol.* **24**, 491–499
11. MacPherson, G. G., Warrell, M. J., White, N. J., Looareesuwan, S., and Warrell, D. A. (1985) Human cerebral malaria. A quantitative ultrastructural analysis of parasitized erythrocyte sequestration. *Am. J. Pathol.* **119**, 385–401
12. Jambou, R., Combes, V., Jambou, M. J., Weksler, B. B., Couraud, P. O., and Grau, G. E. (2010) Plasmodium falciparum adhesion on human brain microvascular endothelial cells involves transmigration-like cup formation and induces opening of intercellular junctions. *PLoS Pathog.* **6**, e1001021
13. Chakravorty, S. J., and Craig, A. (2005) The role of ICAM-1 in *Plasmodium falciparum* cytoadherence. *Eur. J. Cell Biol.* **84**, 15–27
14. Ochola, L. B., Siddondo, B. R., Ocholla, H., Nkya, S., Kimani, E. N., Williams, T. N., Makale, J. O., Liljander, A., Urban, B. C., Bull, P. C., Szestak, T., Marsh, K., and Craig, A. G. (2011) Specific receptor usage in *Plasmodium falciparum* cytoadherence is associated with disease outcome. *PLoS One* **6**, e14741

15. Engwerda, C., Belnoue, E., Grüner, A. C., and Rénia, L. (2005) Experimental models of cerebral malaria. *Curr. Top. Microbiol. Immunol.* **297**, 103–143
16. Feldmeier, J. J. (2003) *Hyperbaric Oxygen 2003: Indications and Results: the Hyperbaric Oxygen Therapy Committee Report*, Undersea and Hyperbaric Medical Society Kensington, Kensington, MD
17. Al-Waili, N. S., Butler, G. J., Beale, J., Abdullah, M. S., Hamilton, R. W., Lee, B. Y., Lucus, P., Allen, M. W., Petrillo, R. L., Carrey, Z., and Finkelstein, M. (2005) Hyperbaric oxygen in the treatment of patients with cerebral stroke, brain trauma, and neurologic disease. *Adv. Ther.* **22**, 659–678
18. Blanco, Y. C., Farias, A. S., Goelnitz, U., Lopes, S. C., Arrais-Silva, W. W., Carvalho, B. O., Amino, R., Wunderlich, G., Santos, L. M., Giorgio, S., and Costa, F. T. (2008) Hyperbaric oxygen prevents early death caused by experimental cerebral malaria. *PLoS One* **3**, e3126
19. Fecher, R. A., Horwath, M. C., Friedrich, D., Rupp, J., and Deepe, G. S., Jr. (2016) Inverse correlation between IL-10 and HIF-1α in macrophages infected with *Histoplasma capsulatum*. *J. Immunol.* **197**, 565–579
20. Lacerda-Queiroz, N., Rodrigues, D. H., Vilela, M. C., Miranda, A. S., Amaral, D. C., Camargos, E. R., Carvalho, L. J., Howe, C. L., Teixeira, M. M., and Teixeira, A. L. (2010) Inflammatory changes in the central nervous system are associated with behavioral impairment in *Plasmodium berghei* (strain ANKA)-infected mice. *Exp. Parasitol.* **125**, 271–278
21. Vignau, J., Jacquemont, M. C., Lefort, A., Imbenotte, M., and Lhermitte, M. (2004) Simultaneous determination of tryptophan and kynurenine in serum by HPLC with UV and fluorescence detection. *Biomed. Chromatogr.* **18**, 872–874
22. Zhang, X., He, Y., and Ding, M. (2009) Simultaneous determination of tryptophan and kynurenine in plasma samples of children patients with Kawasaki disease by high-performance liquid chromatography with programmed wavelength ultraviolet detection. *J. Chromatogr. B Analyt. Technol. Biomed. Life Sci.* **877**, 1678–1682
23. Baptista, F. G., Pamplona, A., Pena, A. C., Mota, M. M., Pied, S., and Vigário, A. M. (2010) Accumulation of *Plasmodium berghei*-infected red blood cells in the brain is crucial for the development of cerebral malaria in mice. *Infect. Immun.* **78**, 4033–4039
24. Howland, S. W., Claser, C., Poh, C. M., Gun, S. Y., and Rénia, L. (2015) Pathogenic CD8+ T cells in experimental cerebral malaria. *Semin. Immunopathol.* **37**, 221–231
25. Howland, S. W., Poh, C. M., Gun, S. Y., Claser, C., Malleret, B., Shastri, N., Ginhoux, F., Grotenbreg, G. M., and Rénia, L. (2013) Brain microvessel cross-presentation is a hallmark of experimental cerebral malaria. *EMBO Mol. Med.* **5**, 984–999
26. Howland, S. W., Poh, C. M., and Rénia, L. (2015) Activated brain endothelial cells cross-present malaria antigen. *PLoS Pathog.* **11**, e1004963
27. Moxon, C. A., Wassmer, S. C., Milner, D. A., Jr., Chisala, N. V., Taylor, T. E., Seydel, K. B., Molyneux, M. E., Faragher, B., Esmon, C. T., Downey, C., Toh, C. H., Craig, A. G., and Heyderman, R. S. (2013) Loss of endothelial protein C receptors links coagulation and inflammation to parasite sequestration in cerebral malaria in African children. *Blood* **122**, 842–851
28. Cabrales, P., Martins, Y. C., Ong, P. K., Zanini, G. M., Frangos, J. A., and Carvalho, L. J. (2013) Cerebral tissue oxygenation impairment during experimental cerebral malaria. *Virulence* **4**, 686–697
29. Hempel, C., Combes, V., Hunt, N. H., Kurtzhals, J. A., and Grau, G. E. (2011) CNS hypoxia is more pronounced in murine cerebral than noncerebral malaria and is reversed by erythropoietin. *Am. J. Pathol.* **179**, 1939–1950
30. Kaur, C., and Ling, E. A. (2008) Blood brain barrier in hypoxic-ischemic conditions. *Curr. Neurovasc. Res.* **5**, 71–81
31. Engelhardt, S., Al-Ahmad, A. J., Gassmann, M., and Ogunshola, O. O. (2014) Hypoxia selectively disrupts brain microvascular endothelial tight junction complexes through a hypoxia-inducible factor-1 (HIF-1) dependent mechanism. *J. Cell. Physiol.* **229**, 1096–1105
32. Jewell, U. R., Kvietikova, I., Scheid, A., Bauer, C., Wenger, R. H., and Gassmann, M. (2001) Induction of HIF-1alpha in response to hypoxia is instantaneous. *FASEB J.* **15**, 1312–1314
33. Sharp, F. R., and Bernaudin, M. (2004) HIF1 and oxygen sensing in the brain. *Nat. Rev. Neurosci.* **5**, 437–448
34. Vorrink, S. U., and Domann, F. E. (2014) Regulatory crosstalk and interference between the xenobiotic and hypoxia sensing pathways at the AhR-ARNT-HIF1α signaling node. *Chem. Biol. Interact.* **218**, 82–88
35. Mascanfroni, I. D., Takenaka, M. C., Yeste, A., Patel, B., Wu, Y., Kenison, J. E., Siddiqui, S., Basso, A. S., Otterbein, L. E., Pardoll, D. M., Pan, F., Priel, A., Clish, C. B., Robson, S. C., and Quintana, F. J. (2015) Metabolic control of type 1 regulatory T cell differentiation by AHR and HIF1-α. *Nat. Med.* **21**, 638–646
36. Otterbein, L. E., Soares, M. P., Yamashita, K., and Bach, F. H. (2003) Heme oxygenase-1: unleashing the protective properties of heme. *Trends Immunol.* **24**, 449–455
37. Lee, P. J., Jiang, B. H., Chin, B. Y., Iyer, N. V., Alam, J., Semenza, G. L., and Choi, A. M. (1997) Hypoxia-inducible factor-1 mediates transcriptional activation of the heme oxygenase-1 gene in response to hypoxia. *J. Biol. Chem.* **272**, 5375–5381
38. Alam, J., and Cook, J. L. (2007) How many transcription factors does it take to turn on the heme oxygenase-1 gene? *Am. J. Respir. Cell Mol. Biol.* **36**, 166–174
39. Neubauer, J. A., and Sunderram, J. (2012) Heme oxygenase-1 and chronic hypoxia. *Respir. Physiol. Neurobiol.* **184**, 178–185
40. Hunt, N. H., and Stocker, R. (2007) Heme moves to center stage in cerebral malaria. *Nat. Med.* **13**, 667–669
41. Nizet, V., and Johnson, R. S. (2009) Interdependence of hypoxic and innate immune responses. *Nat. Rev. Immunol.* **9**, 609–617
42. McBerry, C., Gonzalez, R. M., Shryock, N., Dias, A., and Aliberti, J. (2012) SOCS2-induced proteasome-dependent TRAF6 degradation: a common anti-inflammatory pathway for control of innate immune responses. *PLoS One* **7**, e38384
43. Mezrich, J. D., Fechner, J. H., Zhang, X., Johnson, B. P., Burlingham, W. J., and Bradfield, C. A. (2010) An interaction between kynurenine and the aryl hydrocarbon receptor can generate regulatory T cells. *J. Immunol.* **185**, 3190–3198
44. Hunt, N. H., Too, L. K., Khaw, L. T., Guo, J., Hee, L., Mitchell, A. J., Grau, G. E., and Ball, H. J. (2017) The kynurenine pathway and parasitic infections that affect CNS function. *Neuropharmacology* **112**(Pt B), 389–398
45. Wang, Y., Liu, H., McKenzie, G., Witting, P. K., Stasch, J. P., Hahn, M., Changsirivathanathamrong, D., Wu, B. J., Ball, H. J., Thomas, S. R., Kapoor, V., Celermajer, D. S., Mellor, A. L., Keaney, J. F., Jr., Hunt, N. H., and Stocker, R. (2010) Kynurenine is an endothelium-derived relaxing factor produced during inflammation. [Erratum in *Nat. Med.* (2010) 16, 607] *Nat. Med.* **16**, 279–285
46. Strasser, B., Becker, K., Fuchs, D., and Gostner, J. M. (2017) Kynurenine pathway metabolism and immune activation: peripheral measurements in psychiatric and co-morbid conditions. *Neuropharmacology* **112**(Pt B), 286–296
47. Gazzinelli, R. T., Kalantari, P., Fitzgerald, K. A., and Golenbock, D. T. (2014) Innate sensing of malaria parasites. *Nat. Rev. Immunol.* **14**, 744–757
48. Dorovini-Zis, K., Schmidt, K., Huynh, H., Fu, W., Whitten, R. O., Milner, D., Kamiza, S., Molyneux, M., and Taylor, T. E. (2011) The neuropathology of fatal cerebral malaria in malawian children. *Am. J. Pathol.* **178**, 2146–2158
49. Belnoue, E., Kayibanda, M., Vigario, A. M., Deschemin, J. C., van Rooijen, N., Viguier, M., Snounou, G., and Rénia, L. (2002) On the pathogenic role of brain-sequestered alphabeta CD8+ T cells in experimental cerebral malaria. *J. Immunol.* **169**, 6369–6375
50. Hellwig-Bürgel, T., Rutkowski, K., Metzen, E., Fandrey, J., and Jelkmann, W. (1999) Interleukin-1beta and tumor necrosis factor-alpha stimulate DNA binding of hypoxia-inducible factor-1. *Blood* **94**, 1561–1567
51. Jacob, A., Potin, S., Saubaméa, B., Crete, D., Scherrmann, J. M., Curis, E., Peyssonnaux, C., and Declèves, X. (2015) Hypoxia interferes with aryl hydrocarbon receptor pathway in hCMEC/D3 human cerebral microvascular endothelial cells. *J. Neurochem.* **132**, 373–383
52. Brant, F., Miranda, A. S., Esper, L., Rodrigues, D. H., Kangussu, L. M., Bonaventura, D., Soriani, F. M., Pinho, V., Souza, D. G., Rachid, M. A., Weiss, L. M., Tanowitz, H. B., Teixeira, M. M., Teixeira, A. L., and Machado, F. S. (2014) Role of the aryl hydrocarbon receptor in the immune response profile and development of pathology during *Plasmodium berghei* Anka infection. *Infect. Immun.* **82**, 3127–3140
53. Owe-Young, R., Webster, N. L., Mukhtar, M., Pomerantz, R. J., Smythe, G., Walker, D., Armati, P. J., Crowe, S. M., and Brew, B. J. (2008) Kynurenine pathway metabolism in human blood-brain-barrier cells: implications for immune tolerance and neurotoxicity. *J. Neurochem.* **105**, 1346–1357
54. Schwarcz, R., Bruno, J. P., Muchowski, P. J., and Wu, H. Q. (2012) Kynurenines in the mammalian brain: when physiology meets pathology. *Nat. Rev. Neurosci.* **13**, 465–477

Received for publication August 18, 2017.
Accepted for publication March 5, 2018.